

# High temperature multiferroicity and strong magnetocrystalline anisotropy in $3d-5d$ double perovskites

Marjana Ležaić<sup>1,2</sup> and Nicola A. Spaldin<sup>2</sup>

<sup>1</sup>*Peter Grünberg Institut, Forschungszentrum Jülich, D-52425 Jülich and JARA-FIT, Germany\**

<sup>2</sup>*Department of Materials, ETH Zurich, Wolfgang-Pauli Strasse 27, CH-8093 Zurich, Switzerland*

Using density functional calculations we explore the properties of as-yet-unsynthesized  $3d-5d$  ordered double perovskites ( $A_2BB'O_6$ ) with highly polarizable  $Bi^{3+}$  ions on the  $A$  site. We find that the  $Bi_2NiReO_6$  and  $Bi_2MnReO_6$  compounds are insulating and exhibit a robust net magnetization that persists above room temperature. When the in-plane lattice vectors of the pseudocubic unit cell are constrained to be orthogonal (for example, by coherent heteroepitaxy), the ground states are ferroelectric with large polarization and a very large uniaxial magnetocrystalline anisotropy with easy axis along the ferroelectric polarization direction. Our results suggest a route to multiferroism and electrically controlled magnetization orientation at room temperature.

PACS numbers: 75.85.+t, 77.55.Nv

## INTRODUCTION

There is increasing current interest in developing multiferroic materials with ferromagnetic and ferroelectric order in the same phase for future spintronic or magnetoelectronic devices [1–4]. Although new multiferroics are being predicted and synthesized at an accelerating pace, a major obstacle for their adoption in applications remains their low magnetic ordering temperatures, which are generally far below room temperature. The problem more generally lies in the scarcity of insulators with any net magnetization – either ferro- or ferrimagnetic – at room temperature, even before the additional requirement of polarization is included. Most work on novel multiferroics has been restricted to  $3d$  transition metal oxides (see, for example, Refs. [5–12]), motivated by the expectation that  $4d$  or  $5d$  compounds would likely be metallic. However, recent work on new  $3d-5d$  double perovskites [13, 14] showed this to be a misconception, and identified a ferrimagnetic insulator,  $Sr_2CrOsO_6$ , with magnetic ordering temperature well above room temperature. First-principles calculations have been shown to accurately reproduce the measured magnetic ordering temperatures, [15, 16] in the  $Sr_2CrMO_6$  series ( $M = W, Re, Os$ ), [17] and have been invaluable in explaining the origin of the robust ferrimagnetic ordering. [18–21]

We build here on these recent developments to propose a route to achieving multiferroics with higher magnetic ordering temperatures. We use  $3d-5d$  double perovskites to achieve high temperature magnetism combined with insulating behavior, and introduce lone-pair active cations on the  $A$  sites to induce polarizability [22, 23]. The heavy  $Bi$  and  $5d$  elements provide an additional desirable feature: The spin-orbit interaction strongly couples the magnetic easy axis to the ferroelectric polarization direction. Specifically, we explore two compounds,  $Bi_2MnReO_6$  and  $Bi_2NiReO_6$ . We use density functional theory to calculate their zero Kelvin struc-

ture and magnetic ordering, and Monte Carlo simulations with parameters extracted from the first-principles calculations to calculate their magnetic ordering temperatures. We find that both materials are magnetic insulators, with ordering temperatures well above room temperature. While the global ground state in both materials is anti-polar, we show that when the in-plane lattice vectors form an angle close to  $90^\circ$  a ferroelectric phase results. In practice this could be achieved using coherent heteroepitaxy and the resulting ferroelectricity could be manipulated using strain. We show that the magnetic behavior results from an antiferromagnetic superexchange [17, 24] and the ferroelectricity from the  $Bi^{3+}$  lone pairs, reminiscent of other  $Bi$ -based multiferroics. Finally, we investigate the effect of strong spin-orbit coupling (SOC) due to the presence of heavy  $Bi^{3+}$  and  $Re^{4+}$  cations on the structural, magnetic, and ferroelectric properties of these compounds.

## METHOD OF CALCULATION

Structural optimizations were performed using the Vienna *Ab-initio* Simulation Package (VASP) with projector augmented wave (PAW) potentials; [25] the semicore  $p$  states of  $Mn$ ,  $Ni$ , and  $Re$  and the  $d$  states of  $Bi$  were included in the valence. We used an energy cutoff of 500 eV and  $6 \times 6 \times 6$ ,  $4 \times 4 \times 6$ , and  $4 \times 4 \times 4$   $\Gamma$ -point centered  $k$ -point meshes for unit cells containing 10, 20, and 40 atoms respectively. The exchange-correlation functional was treated within the generalized gradient approximation (GGA); [26] while extension to the GGA+ $U$  method had only a small influence on the electronic properties, we discuss later its effect on the structural behavior. Magnetic ordering temperatures were obtained using a finite-temperature Monte Carlo scheme within a Heisenberg Hamiltonian  $H = -\frac{1}{2} \sum_{i,j} J_{i,j} \mathbf{M}_i \cdot \mathbf{M}_j$ , where  $\mathbf{M}_i$  and  $\mathbf{M}_j$  are the magnetic moments on sites  $i$  and  $j$  of the crystal lattice. The exchange constants  $J_{i,j}$  were cal-

culated in the frozen-magnon scheme [27] using the all-electron full-potential linearized augmented plane-wave code FLEUR [28], with a plane-wave cutoff of 4.2 hartrees and  $15 \times 15 \times 15$   $k$ -points and a  $6 \times 6 \times 6$  spin-spiral grid in a 10-atom unit cell. Ferroelectric polarizations were extracted from the shifts of the centers of Wannier functions [29]. The magnetocrystalline anisotropy energy was extracted from the self-consistent total-energy calculations within the FLEUR code, on a  $13 \times 13 \times 13$   $k$ -point grid.

First, we calculate the lowest energy structure for both  $\text{Bi}_2\text{MnReO}_6$  and  $\text{Bi}_2\text{NiReO}_6$  within the GGA approximation. We proceed by successively freezing in the 12 centrosymmetric combinations of tilts and rotations of the oxygen octahedra that can occur in ordered double perovskites [30]. We then further reduce the symmetry of these lowest energy tilt systems by displacing the anions and cations relative to each other in the manner of a polar displacement. Next we optimize the atomic positions (by minimizing the Hellmann-Feynman forces), as well as the unit cell shape and volume within each symmetry. In this first series of optimizations we assume ferrimagnetic ordering and do not include SOC; the influence of SOC on the lowest-energy structures is examined later.

### GROUND-STATE STRUCTURE AND INFLUENCE OF EPITAXIAL CONSTRAINTS

Our calculations yield the same monoclinic, centrosymmetric  $P2_1/n$  symmetry ground state for both compounds. It is characterized by an  $a^-a^-c^+$  tilt pattern of the oxygen octahedra. Two lattice vectors are identical with angles of  $93.6^\circ$  and  $93.5^\circ$  between them in the Mn and Ni compounds, respectively (in the following we refer to these as the “in-plane” lattice vectors); the third lattice vector is perpendicular to the first two and of different length. Importantly, in both compounds there is a slightly higher energy ferroelectric (FE) structure with rhombohedral  $R\bar{3}$  symmetry (see Table I). The  $R\bar{3}$  structure corresponds to an  $a^-a^-a^-$  tilt pattern yielding lattice vectors of equal length and rhombohedral angles of  $60^\circ$  and  $61^\circ$  for the Mn and Ni compounds respectively, combined with polar relative displacements of anions and cations along the  $[111]$  rhombohedral axis in-

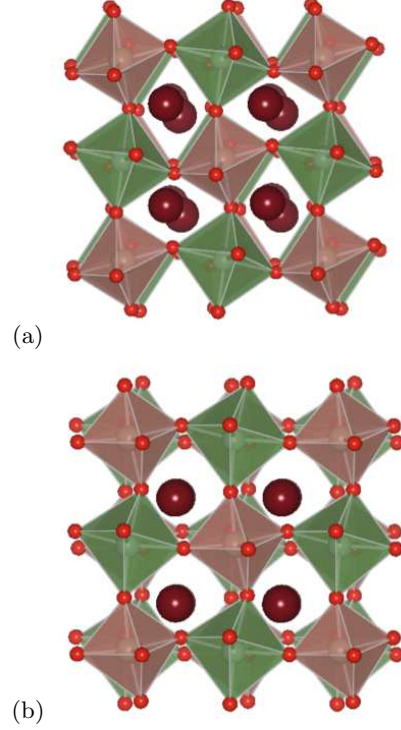


FIG. 1: (Color online) (a) Ground-state  $P2_1/n$  structure and (b) the ferroelectric  $R\bar{3}$  structure of the double perovskites  $\text{Bi}_2\text{MnReO}_6$  and  $\text{Bi}_2\text{NiReO}_6$ .  $\text{Bi}^{3+}$  cations are depicted as the large (brown) spheres and  $\text{O}^{2-}$  as the small (red) spheres.  $\text{Re}^{4+}$  and  $\text{Mn}^{2+}$  ( $\text{Ni}^{2+}$ ) are alternating in the shaded octahedra, in a three-dimensional checkerboard manner (this is indicated by the color of the octahedra). While in the  $P2_1/n$  symmetry the  $\text{Bi}^{3+}$  cations form an “antipolar” pattern, their coherent shift along the  $[111]$  direction can be clearly seen in the  $R\bar{3}$  structure.

duced by the well-established stereochemically active Bi lone pair [22] (see Fig. 1). The energy of the FE phase is significantly lower than that of the corresponding centrosymmetric  $R\bar{3}$  phase, suggesting a high ferroelectric ordering temperature if this symmetry could be stabilized. For comparison, in the prototypical multiferroic  $\text{BiFeO}_3$  with  $T_C$  of 1103 K, we obtain a difference of 515 meV per two formula units between the corresponding states. The calculated polarization in both cases is along the  $[111]$  direction, and comparable in size to that of  $\text{BiFeO}_3$  (see Table II).

While the ground state  $P2_1/n$  phase is of interest in its own right as a possible high temperature magnetic insulator, we next explore whether it is possible to identify conditions that stabilize the  $R\bar{3}$  ferroelectric phase. We use the fact that in the FE  $R\bar{3}$  phase all three lattice vectors have equal length, and the rhombohedral angle is equal or close to the ideal value of  $60^\circ$ . In contrast, in the  $P2_1/n$  phase, only the lengths of the two in-plane lattice vectors are equal, and the inter-in-plane angles deviate

Symmetry	Tilt system	Total energy	
	(in Glazer notation [31])	$\text{Bi}_2\text{MnReO}_6$	$\text{Bi}_2\text{NiReO}_6$
$Fm\bar{3}m$	$a^0a^0a^0$	1.86 eV	2.02 eV
$R\bar{3}$	$a^-a^-a^-$	248 meV	333 meV
$R\bar{3}$	$a^-a^-a^- + \text{FE shift}$	32 meV	18 meV

TABLE I: Total energies (per formula unit) of the lowest-energy phases of  $\text{Bi}_2\text{MnReO}_6$  and  $\text{Bi}_2\text{NiReO}_6$  and the cubic  $Fm\bar{3}m$  phase with respect to their ground state  $P2_1/n$  phase.

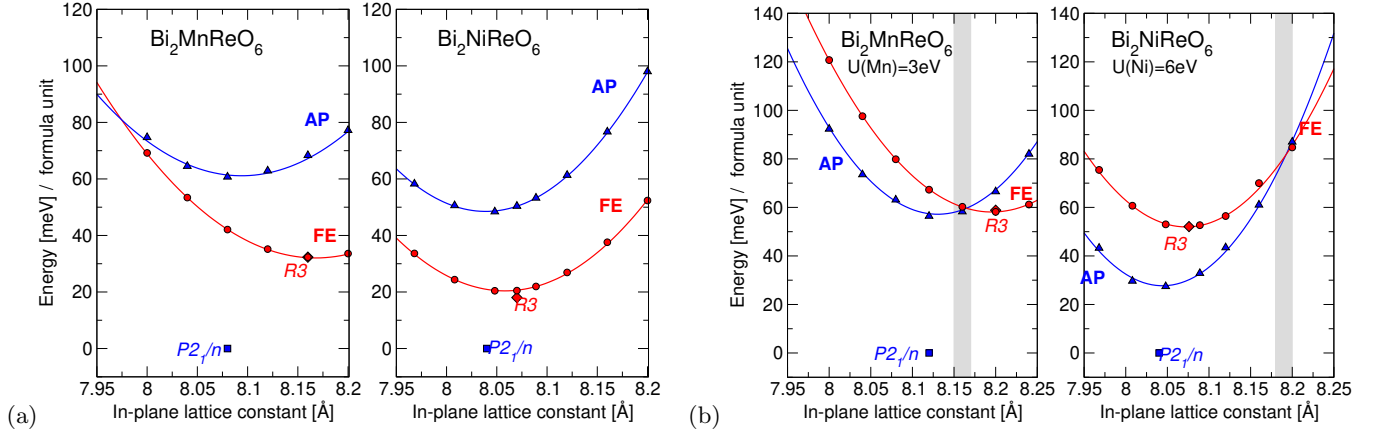


FIG. 2: (Color online) (a) Distorted  $\text{Bi}_2\text{MnReO}_6$  and  $\text{Bi}_2\text{NiReO}_6$  obtained from the  $R3$  (red circles) and  $P2_1/n$  (blue triangles) structure by constraining the two in-plane lattice vectors to be equal and the angle between them to  $90^\circ$ . The out-of-plane parameter and the ionic positions were relaxed. The energies are positioned with respect to the bulk unconstrained  $P2_1/n$  ground state (blue squares). The red diamonds show the energies for the unconstrained  $R3$  structure. A crossover between the antipolar (AP) and the ferroelectric (FE) state occurs at 1.8% (with respect to the minimum of the FE curve) of compressive strain in  $\text{Bi}_2\text{MnReO}_6$ . Note that the energy of the  $R3$  state lies on the strain curve for  $\text{Bi}_2\text{MnReO}_6$ , but is somewhat lower for  $\text{Bi}_2\text{NiReO}_6$ , due to the choice of a square in-plane lattice: the rhombohedral angle in  $R3$  phase of  $\text{Bi}_2\text{MnReO}_6$  is  $60^\circ$ , while in  $\text{Bi}_2\text{NiReO}_6$  it is  $61^\circ$ . (b) Similar to (a), with an addition of a Hubbard  $U$  on Mn (3 eV) and Ni (6 eV) 3d states. The shaded area shows the AP-FE crossover region.

strongly from the ideal  $90^\circ$ . Motivated by these observations, we first constrain all three lattice parameters to be equal in length and indeed find that this constraint stabilizes the FE phase. Next we enforce that only two of the three lattice parameters are equal in length, but constrain them to be perpendicular to each other and again find that the FE phase is the lowest energy [37]. Such a constraint could be achieved in practice through coherent heteroepitaxy between a thin film and a substrate, and is often described as a biaxial strain state in the literature. In Fig. 2(a), we show the calculated energies of the previously  $R3$  and  $P2_1/n$  structure types subject to this additional constraint, with the in-plane lattice parameters varied over a range of realistic substrate strains corresponding to (001) epitaxial growth. For each in-plane lattice parameter we allow the length and angle of the out-of-plane lattice parameter and atomic positions to relax to their lowest-energy configurations. Our main finding is that, under the investigated constraint, the FE phase is lower in energy than the antipolar (AP) phase. At the optimized value of the in-plane lattice parameter (8.16 Å for  $\text{Bi}_2\text{MnReO}_6$  and 8.07 Å for  $\text{Bi}_2\text{NiReO}_6$ ) the energy differences between the FE and AP phases are 36 and 30 meV per formula unit, respectively. The FE phases are robustly insulating with calculated band gaps of 0.7 and 0.3 eV, respectively, and have large polarizations of  $84 \mu\text{C}/\text{cm}^2$  ( $\text{Bi}_2\text{MnReO}_6$ ) and  $81 \mu\text{C}/\text{cm}^2$  ( $\text{Bi}_2\text{NiReO}_6$ ) along the pseudocubic [111] direction. Notice, however, that as in-plane compressive strain is applied, the differences in energies reduce, and in fact in  $\text{Bi}_2\text{MnReO}_6$  a crossover is reached at a compressive strain value of 1.8%.

We therefore expect that both compounds, although AP in bulk, will in fact be ferroelectric and hence multiferroic in thin-film form, over a range of experimentally accessible strains. We see later that SOC tips the scale toward the FE phase, while electron correlations favor the AP phase.

## ELECTRONIC AND MAGNETIC PROPERTIES OF THE FERROELECTRIC PHASE

Next, we analyze the magnetic behavior of the two ferroelectric compounds. We find that in both cases the lowest-energy ordering is ferrimagnetic, with the moments on the 3d and 5d transition metal ions antialigned (see Fig. 3). In both compounds, Re is in formal oxidation state  $4^+$  corresponding to a filled  $d-t_{2g}$  manifold in the minority spin-channel. The oxidation states of Mn in  $\text{Bi}_2\text{MnReO}_6$  and of Ni in  $\text{Bi}_2\text{NiReO}_6$  are  $2^+$ :  $t_{2g}^3 e_g^2$  (high spin) for Mn and  $t_{2g}^6 e_g^2$  for Ni. Due to these specific configurations of the outer electronic shells, and the nearly  $150^\circ$  Mn-O-Re (Ni-O-Re) angle, the magnetic moments on Re and Mn/Ni are coupled via an antiferromagnetic superexchange mechanism. [33–35] The result is a ferrimagnetic configuration with a total spin moment of  $2 \mu_B$  in  $\text{Bi}_2\text{MnReO}_6$  and  $1 \mu_B$  in  $\text{Bi}_2\text{NiReO}_6$ .

Our calculated magnetic ordering temperatures in the ferroelectric phase are 330 K for  $\text{Bi}_2\text{MnReO}_6$  and 360 K for  $\text{Bi}_2\text{NiReO}_6$ , both significantly above room temperature. As a comparison, using the same method, we calculate a magnetic ordering temperature of 670 K for

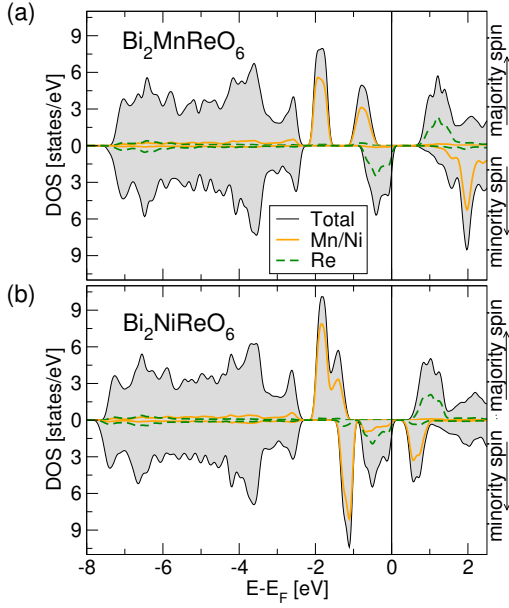


FIG. 3: (Color online) Density of states (DOS) of the ferroelectric phase of  $\text{Bi}_2\text{MnReO}_6$  (a) and  $\text{Bi}_2\text{NiReO}_6$  (b). The local magnetic moments on Mn/Ni and Re are antialigned. Thin black line, total DOS; green dashed line, Re; orange solid line, Mn/Ni.

$\text{Sr}_2\text{CrOsO}_6$  (the experimental value is 725 K). Note that if growth can only be achieved in the form of ultra-thin films, the ordering temperatures will likely be reduced.

### SPIN-ORBIT COUPLING AND CORRELATIONS EFFECTS

Since the heavy Re and Bi atoms in our double perovskites are also likely to exhibit strong SOC, and consequently significant magnetostructural coupling, [18] we repeat our calculations with SOC explicitly included. We find that the ground state remains  $P2_1/n$  AP, but now its energy difference from the FE state with  $R3$  symmetry is reduced to 10 meV in  $\text{Bi}_2\text{MnReO}_6$  and only 2 meV in  $\text{Bi}_2\text{NiReO}_6$ . Both compounds still have semiconducting gaps which are now somewhat reduced while the ferroelectric polarization of the  $R3$  phase is slightly increased (see Table II). The total magnetic moments (spin + orbital) amount to 2.34 and 0.58  $\mu_B$ , respectively. Note that, in contrast to half-metallic ferromagnets where the SOC introduces states in the minority-spin gap yielding a noninteger total magnetic moment, here the noninteger moment is the consequence of the mixing of spin-up and spin-down states (spin is no longer a good quantum number with SOC included), while the gap is preserved.

In both compounds the magnetic easy axis lies along the ferroelectric polarization direction. The associated anisotropy energy is large and comparable to that in cur-

SOC	Compound	Band gap [eV]	$P$ ( $\mu\text{C}/\text{cm}^2$ )	$M$ ( $\mu_B/\text{f.u.}$ )
Off	$\text{Bi}_2\text{MnReO}_6$	0.7	84	2
	$\text{Bi}_2\text{NiReO}_6$	0.3	78	1
On	$\text{Bi}_2\text{MnReO}_6$	0.4	86	2.34
	$\text{Bi}_2\text{NiReO}_6$	0.2	80	0.58

TABLE II: Properties of the bulk ferroelectric  $R3$  phase in  $\text{Bi}_2\text{MnReO}_6$  and  $\text{Bi}_2\text{NiReO}_6$  with and without the SOC included: band gap, ferroelectric polarization  $P$  and the total magnetic moment  $M$  (spin+orbital in case of SOC) per formula unit (f.u.).

rent magnetic recording media: it amounts to 7 and 5.5 meV per formula unit in  $\text{Bi}_2\text{MnReO}_6$  and  $\text{Bi}_2\text{NiReO}_6$ , respectively. This suggests an exciting possibility of electrical control of the magnetization direction.

Finally, we investigate the influence of electronic correlations by adding a Hubbard  $U$  on the  $d$  states of Mn and Ni. In order to reduce the computational effort, we do not include the SOC. We keep in mind, however, that a consequence of its inclusion, as we have seen, is a reduction in the energy of the FE state with respect to the AP one. Introduction of Hubbard  $U$  corrections (on Mn  $U=3$  eV and  $J=0.87$  eV, and on Ni  $U=6$  eV and  $J=0.90$  eV) does not change the ground state structure ( $P2_1/n$  still has the lowest energy). Interesting quantitative changes occur in the strain dependence however [Fig. 2(b)]. While within the GGA the ferroelectricity was robust to the choice of substrate lattice parameters over a likely range of accessible strains provided that the in-plane lattice parameters were constrained to be perpendicular to each other, in GGA+ $U$  we find a cross-over between the FE and AP states at moderate strain values. This suggests the intriguing possibility that an external strain, for example from a piezoelectric substrate [36] could induce a “dipole-flop” transition from a non-polar structure in which the dipoles are antialigned to a ferroelectric one. For the assumed value of  $U$ , the crossover region [shaded area in Fig 2(b)] in  $\text{Bi}_2\text{MnReO}_6$  is within less than 1% from either of the two minima: a small compressive strain will push the system toward the AP state, while a small tensile strain will favor a FE state. In  $\text{Bi}_2\text{NiReO}_6$  the applied  $U$  pushes the AP state lower in energy, but the crossover region to the FE state is still within an experimentally accessible range of 1.5% tensile strain. While we can not make a quantitative prediction, since the relative energies of the AP and the FE state depend strongly on the value of the applied  $U$  correction, within a reasonable range of  $U$  the crossover region lies within 2% strain from the ground state structure.

## CONCLUSION

In summary, we predict from first-principles calculations that the  $3d-5d$  double-perovskite compounds  $\text{Bi}_2\text{MnReO}_6$  and  $\text{Bi}_2\text{NiReO}_6$  are high- $T_C$  ferrimagnetic insulators. Moreover, it is likely possible to stabilize them in thin-film form in a ferroelectric phase with high polarization along the  $[111]$  direction. The magnetic easy axis lies along the ferroelectric polarization direction with a very large associated anisotropy energy. The different sizes and charges of the  $3d$  and  $5d$  transition metal ions suggest that the required  $B$ -site ordering should be experimentally feasible; we hope that our findings will initiate experimental efforts to synthesize these novel multiferroic compounds.

We thank Drs. Kris Delaney, Phivos Mavropoulos, Stefan Blügel, Frank Freimuth and Sergey Ivanov for many valuable discussions. M.L. gratefully acknowledges the support of Deutsche Forschungsgemeinschaft, grant LE 2504/1-1, and the Young Investigators Group Programme of Helmholtz Association, contract VH-NG-409, as well as the Jülich Supercomputing Centre. NS acknowledges support from the NSF NIRT program, grant number 0609377.

---

\* Electronic address: m.lezaic@fz-juelich.de

- [1] Xi Chen, A. Hochstrat, P. Borisov, and W. Kleemann, Appl. Phys. Lett. **89**, 202508 (2006).
- [2] M. Gajek, M. Bibes, S. Fusil, K. Bouzehouane, J. Fontcuberta, A. Barthélémy, and A. Fert, Nature Mat. **6**, 296 (2007).
- [3] Ying-Hao Chu, Lane W. Martin, Mikel B. Holcomb, Martin Gajek, Shu-Jen Han, Qing He, Nina Balke, Chan-Ho Yang, Donkoun Lee, Wei Hu, Qian Zhan, Pei-Ling Yang, Arantxa Fraile-rodrguez, Andreas Scholl, Shan X. Wang and R. Ramesh, Nature Mat. **7**, 478 (2008).
- [4] D. Lebeugle, A. Mougin, M. Viret, D. Colson, and L. Ranno, Phys. Rev. Lett. **103**, 257601 (2009)
- [5] Kunihiro Yamauchi, Tetsuya Fukushima, and Silvia Picozzi, Phys. Rev. **79**, 212404 (2009).
- [6] S. Picozzi, K. Yamauchi, B. Sanyal, I. A. Sergienko, and E. Dagotto, Phys. Rev. Lett. **99**, 227201 (2007)
- [7] Gianluca Giovannetti, Sanjeev Kumar, Jeroen van den Brink, and Silvia Picozzi, Phys. Rev. Lett. **103**, 037601 (2009)
- [8] Y. Yamasaki, S. Miyasaka, Y. Kaneko, J.-P. He, T. Arima and Y. Tokura, Phys. Rev. Lett. **96**, 207204 (2006)
- [9] P. Baettig, C. Ederer, and N. A. Spaldin, Phys. Rev. B **72**, 214105 (2005).
- [10] R. Nechache, C. Harnagea, L.-P. Carignan, O. Gautreau, L. Pintilie, M. P. Singh, D. Menard, P. Fournier, M. Alexe, and A. Pignolet, J. Appl. Phys. **105**, 061621 (2009).
- [11] A. J. Hatt, N. A. Spaldin and C. Ederer, Phys. Rev. B **81**, 054109 (2010).
- [12] M. Sakai, A. Masuno, D. Kan, M. Hashisaka, K. Takata, M. Azuma, M. Takano, and Y. Shimakawa, Appl. Phys. Lett. **90**, 072903 (2007)
- [13] Y. Krockenberger, K. Mogare, M. Reehuis, M. Tovar, M. Jansen, G. Vaitheeswaran, V. Kanchana, F. Bultmark, A. Delin, F. Wilhelm, A. Rogalev, A. Winkler, and L. Alff, Phys. Rev. B **75**, 020404R (2007).
- [14] K.-W. Lee and W. E. Pickett, Phys. Rev. B **77**, 115101 (2008).
- [15] J. B. Philipp, P. Majewski, L. Alff, A. Erb, R. Gross, T. Graf, M. S. Brandt, J. Simon, T. Walther, W. Mader, D. Topwal, and D. D. Sarma, Phys. Rev. B **68**, 144431 (2003).
- [16] H. Kato, T. Okuda, Y. Okimoto, Y. Tomioka, Y. Takenoya, A. Ohkubo, M. Kawasaki, and Y. Tokura, Appl. Phys. Lett. **81**, 328 (2002).
- [17] Tapas Kumar Mandal, Claudia Felser, Martha Greenblatt, and Jürgen Kübler, Phys. Rev. B **78**, 134431 (2008).
- [18] D. Serrate, J. M. De Teresa and M. R. Ibarra, J. Phys.:Condens.Matter **19**, 023201 (2007).
- [19] D. D. Sarma, P. Mahadevan, T. Saha-Dasgupta, S. Ray, and A. Kumar, Phys. Rev. Lett. **85**, 2549 (2000).
- [20] J. Kanamori and K. Terakura, J. Phys. Soc. Jpn. **70**, 1433 (2001).
- [21] Z. Fang, K. Terakura, and J. Kanamori, Phys. Rev. B **63**, 180407(R) (2001).
- [22] N. A. Hill and K. M. Rabe, Phys. Rev. B **59**, 8759 (1999).
- [23] R. Seshadri, N. A. Hill, Chem. Mater. **13**, 2892 (2001)
- [24] P. W. Anderson, Phys. Rev. **79**, 350 (1950).
- [25] *The Vienna ab-initio simulation package*, G. Kresse and J. Hafner, Phys. Rev. B **47**, R558 (1993); G. Kresse, Thesis, Technische Universität Wien (1993); G. Kresse and J. Furthmüller, Comput. Mat. Sci. **6**, 15 (1996); G. Kresse and J. Furthmüller, Phys. Rev. B **54**, 11169 (1996); G. Kresse, and D. Joubert, Phys. Rev. B **59**, 1758 (1999); P.E. Blöchl, Phys. Rev. B **50**, 17953 (1994).
- [26] J. P. Perdew, K. Burke, and M. Ernzerhof, Phys. Rev. Lett. **77**, 3865 (1996).
- [27] M. Lezaic, PhD Thesis, RWTH Aachen (2005) [<http://darwin.bth.rwth-aachen.de/opus/volltexte/2006/1359/>].
- [28] www.flapw.de
- [29] F. Freimuth, Y. Mokrousov, D. Wortmann, S. Heinze, and S. Blügel, Phys. Rev. B **78**, 035120 (2008).
- [30] C. J. Howard, B. J. Kennedy, and P. M. Woodward, Acta Cryst. B **59**, 463 (2003).
- [31] A. M. Glazer, Acta Cryst. B **28**, 3384 (1972)
- [32] P. Baettig and N. A. Spaldin, Appl. Phys. Lett. **86**, 012505 (2004).
- [33] J. B. Goodenough, Phys. Rev. **100**, 564 (1955).
- [34] J. Kanamori, J. Phys. Chem. Solids **10** 87 (1959).
- [35] E. O. Wollan, Phys. Rev. **117**, 387 (1960).
- [36] A. D. Rata, A. Herklotz, K. Nenkov, L. Schultz, and K. Dörr, Phys. Rev. Lett. **100**, 076401 (2008).
- [37] Note that the lowest energy  $P2_1/n$  structure would not be readily identified as the ground state through a search for unstable phonons starting from the prototype cubic perovskite structure because it only becomes lowest in energy when the lattice parameters are allowed to be unequal. Indeed, when we perform full structural optimizations within the LDA+U method for the previously studied double perovskite,  $\text{Bi}_2\text{FeCrO}_6$  [32], we find the  $P2_1/n$  structure to be lower in energy than the previously reported  $R3$  when we allow for lattice parameters of different length. Interestingly, in this case, the GGA+U method yields a ferroelectric ground state, con-

sistent with some experimental reports [10].